Reprinted from
Journal of Imaging Science and Technology® 65(6): 060406-1–060406-14, 2021.
© Society for Imaging Science and Technology 2021

Glossy Appearance Editing for Heterogeneous Material Objects

Yusuke Manabe
Graduate School of Science and Engineering, Chiba University, Japan

Midori Tanaka▲
Graduate School of Global and Transdisciplinary Studies, Chiba University, Japan
E-mail: midori@chiba-u.jp

Takahiko Horiuchi▲
Graduate School of Science and Engineering, Chiba University, Japan

Abstract. *With the proliferation of smartphones and social networking services, the opportunities for individuals to take photographs have increased exponentially. In a previous study, the perceived gloss of an object was reduced by its representing as a digital image and compared with a real object. It is also known that image editing, such as lossy image compression, can reduce the glossiness of an image. Therefore, the glossiness of real objects may be easily changed in digital images; thus, a method for appropriately editing the gloss in digital images is required for post-processing. In this study, we propose a gloss appearance editing method for various material objects in a single digital image. The proposed method consists of three steps: color space conversion, gloss detection, and gloss editing. The relationship between the proposed method and the respective reflection models of inhomogeneous objects, metallic objects, and translucent objects was analyzed. Consequently, we determined that the gloss editing of the proposed method is equivalent to editing the specular reflection component of an inhomogeneous object, the grazing reflection component of a metallic object, and the specular reflection component of a translucent object. We applied the proposed method to test images including objects of various materials and confirmed its effectiveness through a subjective evaluation by visual inspection and an objective evaluation using image statistics.* © *2021 Society for Imaging Science and Technology.*
[DOI: 10.2352/J.ImagingSci.Technol.2021.65.6.060406]

1. INTRODUCTION

Just as all objects have color, all objects have certain amount of gloss. Gloss is a surface attribute that provides either a shiny or matte finish, and influences the appearance of a product. The last decade or so has seen a renewal of interest in the perception of gloss, in an effort to map what is now understood to be a complex interaction of variables including illumination, surface properties and the observer. This appears to have been driven by a number of factors, as the study of gloss emerged from research in other surface properties such as color and texture, with technological advances paving the way for new experimental techniques and measurements [1].

A method exists for evaluating the gloss of an object surface using a specular glossmeter. However, specular gloss measurements and visual gloss appraisal do not coincide [2]. Leloup et al. investigated the effect of lighting geometry and luminance contrast on gloss perception using a paired comparison method [3, 4]. The results showed that in addition to the surface properties of the sample, the important factors determining the gloss perception included the shape of the illumination, clarity of the image, and difference in luminance between the specular highlights and the diffuse background. Cheeseman et al. focused on changes in surface reflectance and investigated the changes in gloss perception in response to differences in specular reflection. They focused on the change in surface reflectance and showed that gloss sensitivity depends on the magnitude of the change in the image produced by the different reflectance values [5]. As described above, studies have shown that gloss perception is closely related to a variety of factors.

With the prevalence of services using digital content, opportunities for individuals to take photographs have dramatically increased. Research has been actively conducted to reproduce accurately the material appearance of an image. In general, captured image data are compressed before they are stored or transferred. JPEG, an international standard coding method, is actively used in a variety of media [6]. Although gloss is an important property that expresses the material appearance of an object, Tanaka et al. showed that glossiness can deteriorate in JPEG image coding [7]. They also showed that even if a glossy object is faithfully reproduced in terms of color, brightness, and size on a display, the glossiness may deteriorate depending on the material [8]. In addition, if the exposure level is too high, the gloss becomes stronger, and the material appearance is altered during the reproduction of the image. As shown in the example in Figure 1, overexposure causes the large, flat highlights on the surface of the banana to look like a plastic material. However, few studies have been conducted to properly reproduce the material appearance, such as the gloss, of an object in an image. Therefore, there

▲ IS&T Members.

Received July 21, 2021; accepted for publication Nov. 4, 2021; published online Nov. 19, 2021. Associate Editor: Jean Baptiste Thomas.
1062-3701/2021/65(6)/060406/14/$25.00

Figure 1. An example of the transformation of perceived material due to overexposure.

is need for a method to edit the gloss of an object in a digital image.

Tanaka et al. proposed "PuRet," a method for editing the material appearance in an image [9]. This method focuses on the physiological phenomenon in which the pupil diameter contracts when humans focus on the material appearance, and designs the tone mapping function of the entire image according to the characteristics of the display. Using PuRet, although it is possible to emphasize the material appearance of the entire image, it is impossible to focus on a specific characteristic of a material such as gloss and edit that characteristic. An example of a conventional method that focuses on glossy editing in an image is "band-sifting," proposed by Boyadzhiev et al. [10]. They showed that a subband in the spatial frequency of an image can represent specific appearance information and indicated how this information can be edited by increasing and decreasing these subband signals. Each subband image is obtained by applying an edge-preserving smoothing filter to the luminance component of the original image, and then calculating the difference between the images before and after the smoothing process. By decomposing the frequency components obtained based on frequency, amplitude, and sign, eight types of components can be obtained. By amplifying or attenuating these eight components, it is possible to manipulate not only the glossiness, but also various other appearances. However, the operation requires a trial-and-error approach during the editing process because the physical functioning of the method is not clearly understood.

In this paper, we propose a method for editing the gloss of various material objects in an image based on physical reflection models. The materials we focus on in this study are inhomogeneous dielectrics, metallic objects, and translucent objects.

2. PROPOSED METHOD

With the proposed method, the color space is first converted, as described in Section 2.1. The RGB information obtained from the input image is then converted into HSI information. The gloss components are then detected based on the HSI information obtained, as indicated in Section 2.2. By editing the gloss information obtained, the visual appearance changes, as described in Section 2.3.

2.1 *Color Space Transformation*

The RGB color space of the input image is converted into the HSI color space. We referred to [11] for the following HSI conversion process:

$$\begin{pmatrix} I_x \\ I_y \\ I_z \end{pmatrix} = \begin{pmatrix} 1 & -\frac{1}{2} & -\frac{1}{2} \\ 0 & \frac{\sqrt{3}}{2} & -\frac{\sqrt{3}}{2} \\ \frac{1}{3} & \frac{1}{3} & \frac{1}{3} \end{pmatrix} \begin{pmatrix} R \\ G \\ B \end{pmatrix}, \tag{1}$$

where $(RGB)^T$ is the RGB color value of a pixel represented as a three-dimensional vector, and $\left(I_x I_y I_z\right)^T$ is the converted opponent color signal. Here, the $I_x - I_y$ plane represents the chromaticity component and I_z represents the luminance component. From $\left(I_x I_y I_z\right)^T$, the hue, saturation, and intensity are derived as follows:

$$\text{hue} = \arctan \frac{I_y}{I_x}, \tag{2}$$

$$\text{saturation} = \sqrt{I_x^2 + I_y^2}, \tag{3}$$

$$\text{intensity} = I_z. \tag{4}$$

This color space is similar to the S space defined by Bajcsy et al. [12]. In the S space, the mapping is applied based on the weight of the specified function of the spectrum; however, in this color space, direct conversion from an RGB color space is realized.

2.2 *Gloss Detection*

For gloss detection, we modified the separation method of the specular reflection component [13]. Gloss detection, as shown in Eqs. (3) and (4), is conducted in the saturation–intensity space. Therefore, as a pre-processing step, the clustering of pixels in an image is executed based on the hue information, and the input image is divided into objects with the same hue component.

The pixels are clustered using the property in which the hue of the pixels on the surface of an object with the same reflective properties is determined without being affected by the intensity of the gloss. The properties of the hue components are described in Section 3. First, a 2D Gaussian filter is applied to each RGB channel of the input image to obtain a smoothed image. The hue values are then calculated from the smoothed image using Eq. (2), and a histogram is created. An evaluation was conducted for each hue value, and the image was divided based on the hue with the highest evaluation. In this study, to reduce the variance within clusters and increase the variance between clusters, the evaluation was calculated as follows:

$$\text{evaluation} = \frac{\sigma_b^2}{\sigma_w^2} \tag{5}$$

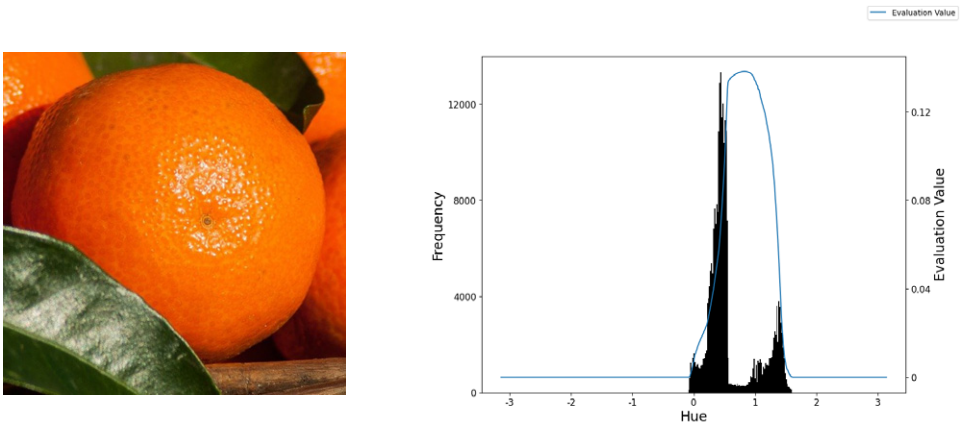

(a) Input image

(b) Histogram and evaluation value

(c) Result of divided image including fruit

(d) Result of divided image including leaves

Figure 2. Clustering results. (a) input image; (b) histogram and evaluation value; (c) result of divided image including fruit; (d) result of divided image including leaves.

where σ_b^2 represents the inter-cluster variance and σ_w^2 represents the intra-cluster variance. These variances can be calculated as follows:

$$\sigma_b^2 = \frac{\omega_1\omega_2\,(m_1 - m_2)^2}{(\omega_1 + \omega_2)^2}, \tag{6}$$

$$\sigma_w^2 = \frac{\omega_1\sigma_1^2 + \omega_2\sigma_2^2}{\omega_1 + \omega_2}, \tag{7}$$

where ω_1 is the number of pixels, m_1 is the mean value, and σ_1^2 is the variance with a hue value smaller than the value of interest; ω_2 is the number of pixels, m_2 is the mean value, and σ_2^2 is the variance with a hue value larger than the value of interest. The process is repeated for the divided area, and finally, the images divided according to the hue information can be obtained. An example of clustering using this process for an image containing fruit is shown in Figure 2. This process divides the image into orange and green leaf regions. The following gloss detection process was applied to segmented images.

Gloss detection is conducted by mapping into the saturation–intensity space. All pixels are separated into groups of pixels with and without gloss. Here, weak gloss pixels exhibit linearity in the saturation–intensity space. In general, saturation can be determined independently of the specular component. In addition, the intensity is constant when the specular reflection component is excluded. Therefore, considering pixels that only possess diffuse reflection components, saturation is proportional to intensity. A detailed explanation is provided in Section 3.1. In addition, the intensity of the pixels with gloss components increases according to the degree of gloss. The details are provided in Section 3. These properties can be used for the approximation of weak gloss pixels as a straight line within the saturation–intensity space, and pixels located around the approximated line are defined as a group of non-glossy pixels. In contrast, pixels distant from the approximated line are defined as gloss pixels. Therefore, the gloss component is obtained as follows:

$$\text{gloss} = \text{intensity} - (G \cdot \text{saturation} + I), \tag{8}$$

where G is the slope and I is the intercept of the approximate straight line. Pixels around and away from the approximate line are classified as glossy and non-glossy pixels, respectively, using a line parallel to the approximate line as a threshold. The threshold value can be used to

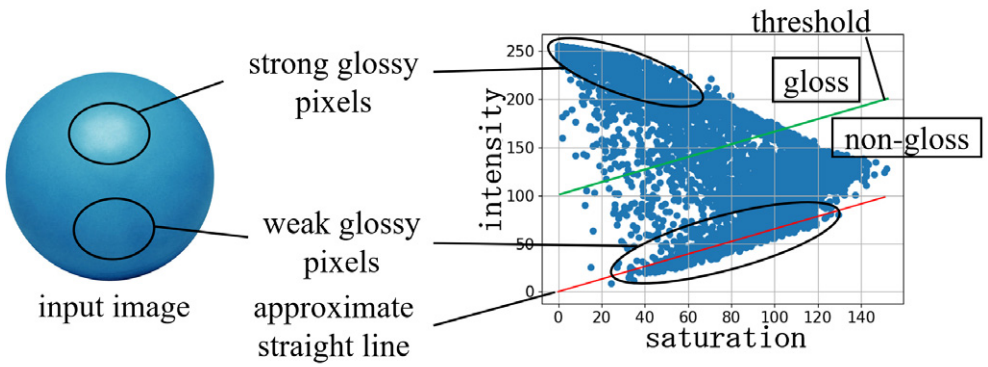

Figure 3. Glossy and non-glossy components in saturation–intensity space.

select the intensity of the gloss to be edited; for example, a high threshold value allows only the components with the highest gloss to be edited. In this study, the threshold was experimentally set to 10. Figure 3 qualitatively illustrates the distribution of the pixels in the two characteristic regions of the input image in the S-I plane.

The approximated line can be derived from the following procedure: First, saturation values are divided at regular intervals α, and the pixel with the minimum intensity is sampled within each interval. If the intensity of the sampled pixel is higher than the average value of the overall intensity value, it is excluded from the list as a glossy pixel. The sampled pixels are approximated using the least-square method. The two parameters of the approximated line are stably derived iteratively by excluding sampled pixels that deviate significantly from the approximated line. The threshold is experimentally set to 30.

2.3 *Gloss Editing*

The gloss components described in Section 2.2 are edited using

$$\text{gloss}' = \text{scale}\left(\text{gloss}, a\right) \cdot \text{gloss}, \tag{9}$$

where gloss and gloss' represent the intensity of the gloss component before and after editing, respectively. In addition, scale $\left(\text{gloss}, a\right)$ is a scale factor, where gloss is a constant and a is a variable. Gloss is enhanced when scale $\left(\text{gloss}, a\right) > 1.0$, and is suppressed when scale $\left(\text{gloss}, a\right) < 1.0$. The value of scale $\left(\text{gloss}, a\right)$ can be arbitrarily designed. In this study, we defined the following:

$$\text{scale}\left(\text{gloss}, a\right) = a \cdot \text{gloss}^2 + 1.0. \tag{10}$$

This scale factor is designed such that pixels with a high gloss intensity are significantly enhanced and areas with low gloss do not change much. By altering the constant a, the degree of gloss enhancement and suppression can be changed.

3. RELATIONSHIP WITH REFLECTION MODELS

In this section, we discuss the relationship between the proposed gloss editing method in the previous section and the reflective properties of various object surfaces within the image. In this study, inhomogeneous, metallic, and translucent objects were all considered, as described in Sections 3.1, 3.2, and 3.3, respectively.

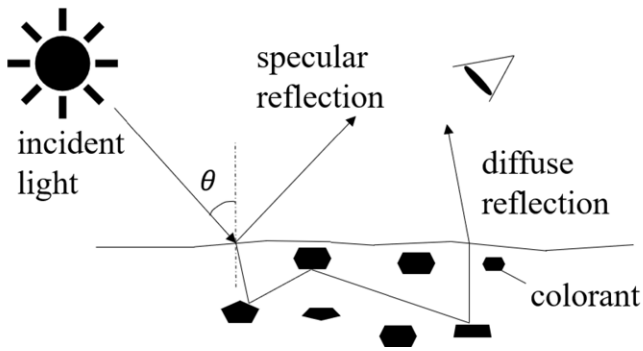

Figure 4. Light reflection process of an inhomogeneous material.

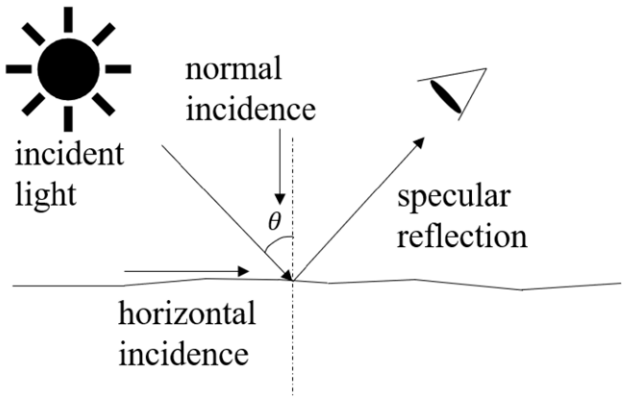

Figure 5. Light reflection process of a metallic material.

3.1 *Inhomogeneous Objects*

In inhomogeneous objects, the layers near the surface of the object are composed of different components, such as vehicles and colorants. Plastic is a typical example of an inhomogeneous object. Tominaga et al. confirmed that the reflection of an inhomogeneous object can be described using a standard dichromatic reflection model and

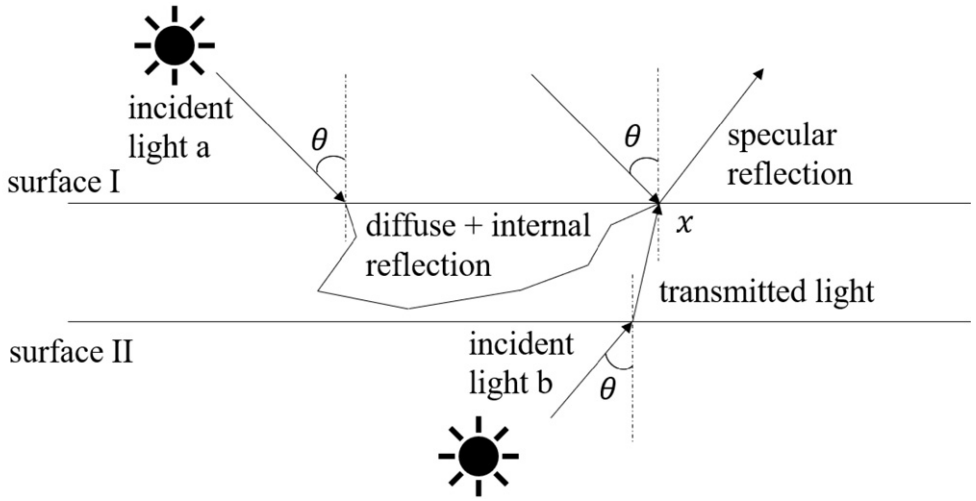

Figure 6. Assumed reflection and transmission model of *translucent* objects.

consists of two types of reflection components, as shown in Figure 4 [14]. The first component is the specular reflection component, in which the incident light is reflected at the boundary between the object surface and the air. The second component is the diffuse reflection component, which occurs when the incident light enters the object, is repeatedly reflected and absorbed, and passes from the object into the air. In the standard dichromatic reflection model, the spectral reflectance $S(\theta, \lambda)$ on the surface of an object is expressed through the following equation:

$$(\theta, \lambda) = c_D(\theta)\, S_D(\lambda) + c_S(\theta), \tag{11}$$

where $c_D(\theta)$ and $c_S(\theta)$ represent the geometric scale factors at incident angle θ, and $S_D(\lambda)$ represents the spectral reflectance of the diffuse reflection component at wavelength λ. In other words, the first term on the right-hand side represents the diffuse reflection component, and the second term denotes the specular reflection component. Equation (11) is expressed as an RGB three-dimensional vector as follows:

$$\begin{pmatrix} R \\ G \\ B \end{pmatrix} = \begin{pmatrix} \gamma_R \\ \gamma_G \\ \gamma_B \end{pmatrix} \cos\theta + \text{specular} \begin{pmatrix} 1 \\ 1 \\ 1 \end{pmatrix}, \tag{12}$$

where $(\gamma_R \gamma_G \gamma_B)^T$ represents the reflectance of the diffuse reflection component in the RGB color space. The variable *specular* represents the intensity of the specular reflection component. Here, we assume that the light source is white, $(111)^T$, and the surface exhibits a Lambertian reflectance. If the light source is not white, the white balance can be changed by setting the elements of the specular reflection vector instead of $(111)^T$.

Each pixel represented by Eq. (12) has the following hue, saturation, and intensity using Eqs. (1)–(4):

$$\text{hue} = \arctan\left(\frac{\frac{\sqrt{3}}{2}\gamma_G - \frac{\sqrt{3}}{2}\gamma_B}{\gamma_R - \frac{1}{2}\gamma_G - \frac{1}{2}\gamma_B}\right), \tag{13}$$

$$\text{saturation} = \frac{\cos\theta}{\sqrt{2}}\sqrt{(\gamma_R - \gamma_G)^2 + (\gamma_G - \gamma_B)^2 + (\gamma_B - \gamma_R)^2}, \tag{14}$$

$$\text{intensity} = \frac{\gamma_R + \gamma_G + \gamma_B}{3}\cos\theta + \text{specular}. \tag{15}$$

Based on Eqs. (13) and (14), hue and saturation were respectively determined independently of the variable *specular*. From Eq. (15), the intensity value increases when the specular reflection component is included. When considering pixels with only the diffuse reflection components from Eqs. (14) and (15), the relationship between the saturation and intensity is proportional, as shown below:

$$\text{intensity} = \frac{\sqrt{2}}{3} \frac{\gamma_R + \gamma_G + \gamma_B}{\sqrt{(\gamma_R - \gamma_G)^2 + (\gamma_G - \gamma_B)^2 + (\gamma_B - \gamma_R)^2}} \cdot \text{saturation}. \tag{16}$$

From the above, with the proposed method, the intensity of the specular reflection component in the standard dichromatic reflection model is detected as a gloss for inhomogeneous objects.

3.2 *Metallic Objects*

The reflection from a metallic object can be represented using the extended dichromatic reflection model for metals, as shown in Figure 5 [15]. According to the reflection model, the reflection of a metallic object is composed of two types of specular reflection components. The first component is the specular reflection at normal incidence, which produces the major object color of a metallic surface. The second component is constant on the wavelength, which corresponds to the grazing reflection at the horizontal incidence where the spectral reflectance is whited. The model assumes that the surface-spectral reflectance function at any incident angle is expressed by combining these two extremes. In the extended dichromatic reflection model, the specular

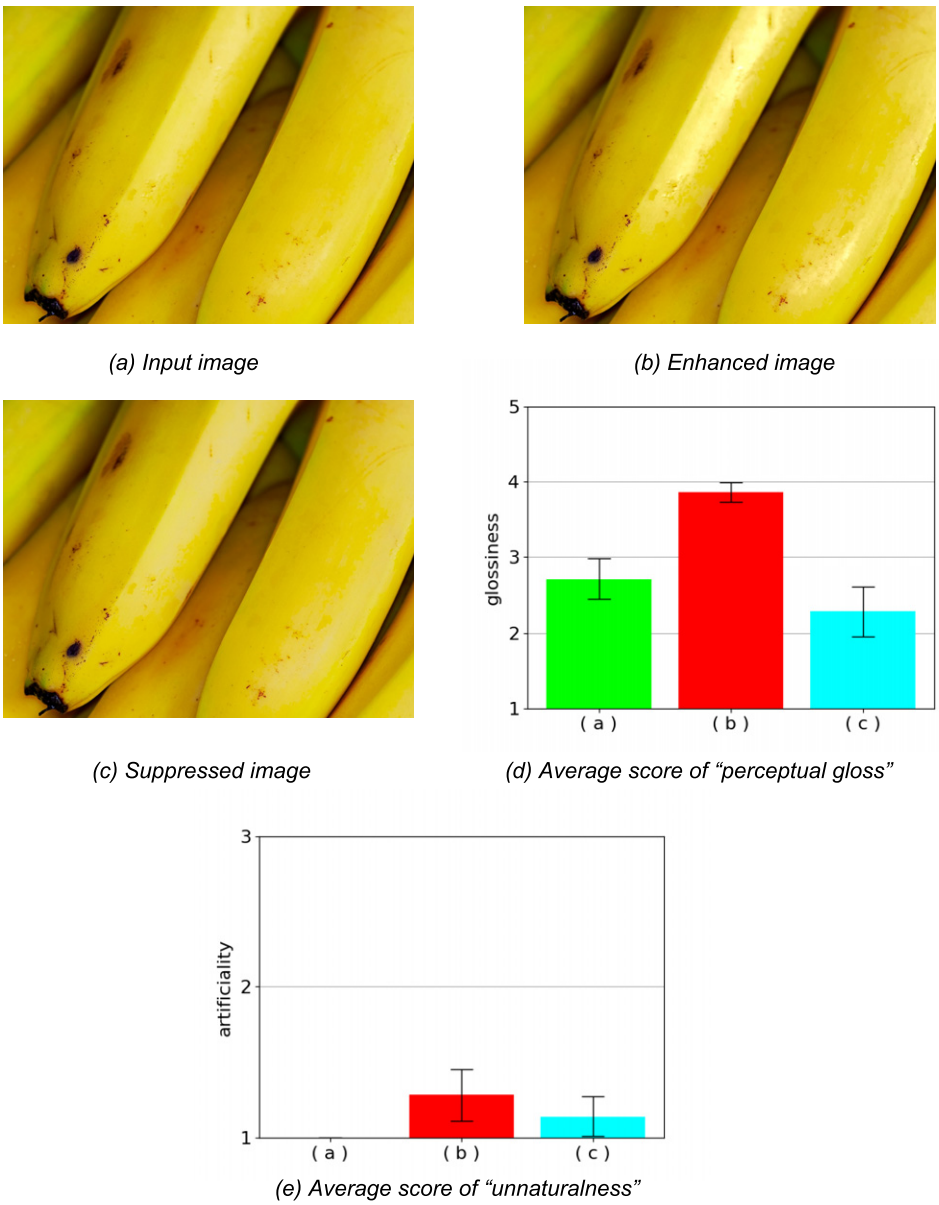

Figure 7. Results of glossy appearance editing for ''banana.'' (a) input image; (b) enhanced image; (c) suppressed image; (d) average score of ''perceptual gloss''; (e) average score of ''unnaturalness''.

reflectance $S(\theta, \lambda)$ on the surface of an object is expressed through the following equation:

$$S(\theta, \lambda) = c_{S1}(\theta)\, S_S(\lambda) + c_{S2}(\theta), \tag{17}$$

where $c_{S1}(\theta)$ and $c_{S2}(\theta)$ represent the geometric scale factors at the incident angle θ, and $S_S(\lambda)$ represents the specular reflectance at normal incidence. That is, the first term on the right-hand side represents the specular reflectance at normal incidence, and the second term denotes the grazing reflection component. Equation (17) is expressed as an RGB three-dimensional vector as follows:

$$\begin{pmatrix} R \\ G \\ B \end{pmatrix} = c_{S1}(\theta) \begin{pmatrix} \mu_R \\ \mu_G \\ \mu_B \end{pmatrix} + c_{S2}(\theta) \begin{pmatrix} 1 \\ 1 \\ 1 \end{pmatrix}, \tag{18}$$

where $(\mu_R \mu_G \mu_B)^T$ represents the specular reflection at normal incidence in the RGB color space. Here, $c_{S2}(\theta)$ represents the intensity of the grazing reflection component.

Each pixel represented by Eq. (18) has the same hue, saturation, and intensity properties as those of the inhomogeneous objects. Therefore, with the proposed method, the intensity of the grazing reflection component is detected as gloss for metallic objects. Because the grazing reflection component is white, and the normal incidence component–which is the major color of the object–does not change, gloss editing is possible without changing the color particular to the object.

3.3 *Translucent Objects*

The reflection and transmission models for translucent objects are illustrated in Figure 6. As shown in the figure,

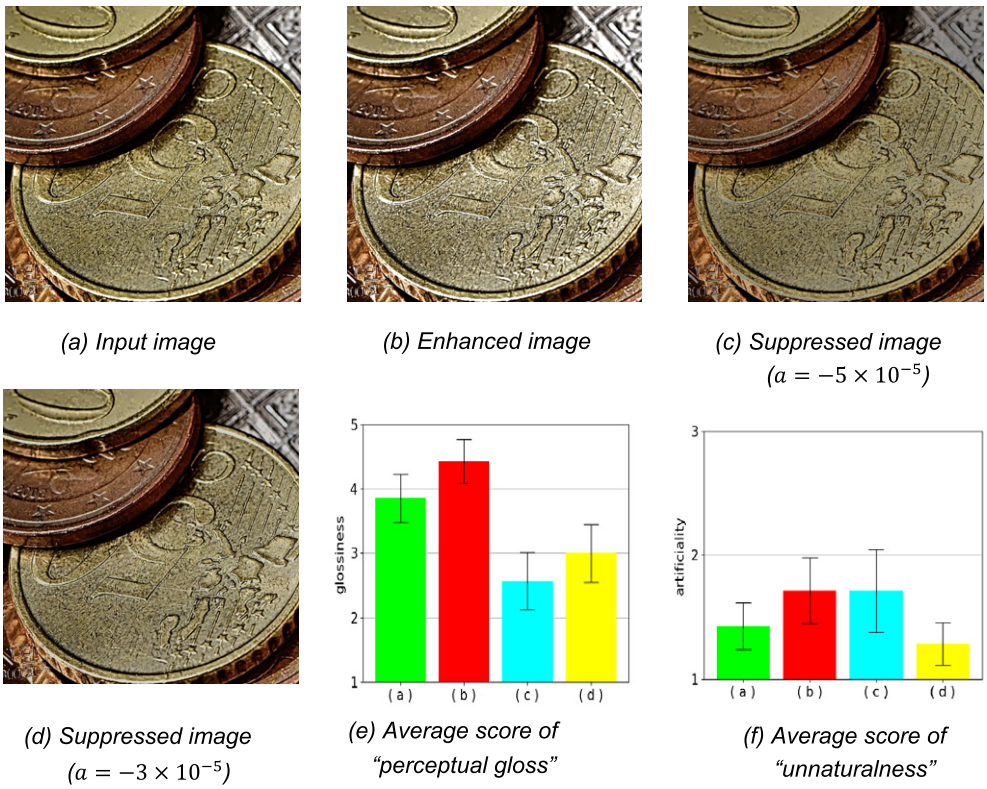

(a) Input image (b) Enhanced image (c) Suppressed image ($a = -5 \times 10^{-5}$)

(d) Suppressed image ($a = -3 \times 10^{-5}$) (e) Average score of "perceptual gloss" (f) Average score of "unnaturalness"

Figure 8. Results of glossy appearance editing for "coins." (a) input image; (b) enhanced image; (c) suppressed image ($a = -5 \times 10^{-5}$); (d) suppressed image ($a = -3 \times 10^{-5}$); (e) average score of "perceptual gloss"; (f) average score of "unnaturalness".

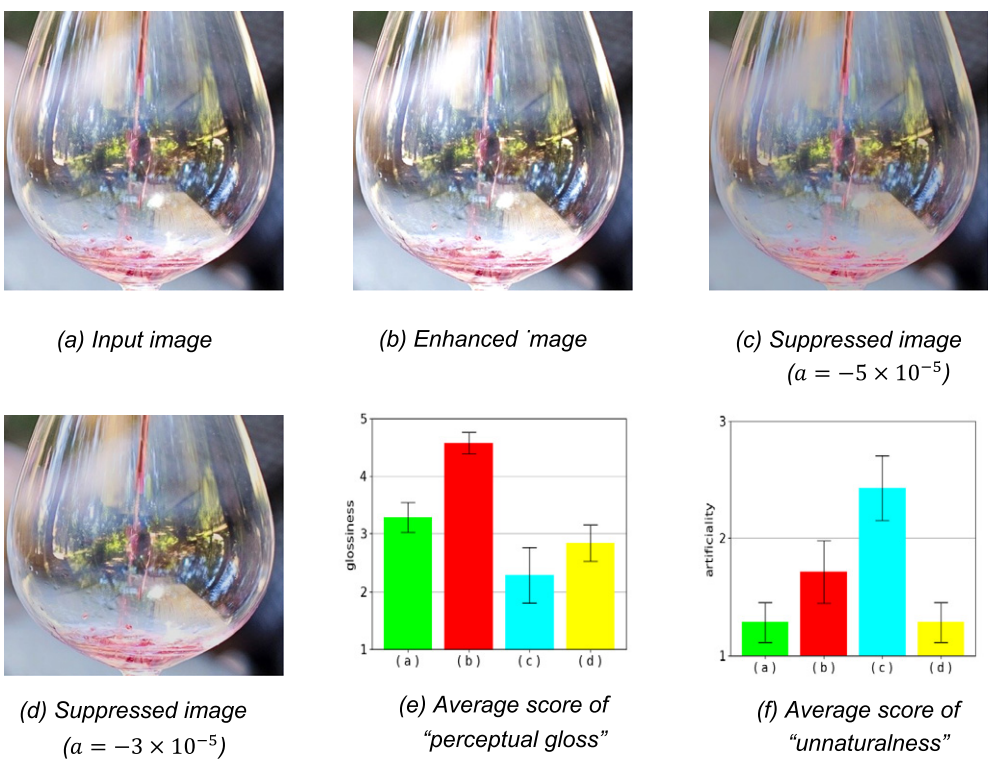

(a) Input image (b) Enhanced image (c) Suppressed image ($a = -5 \times 10^{-5}$)

(d) Suppressed image ($a = -3 \times 10^{-5}$) (e) Average score of "perceptual gloss" (f) Average score of "unnaturalness"

Figure 9. Results of glossy appearance editing for "glass." (a) input image; (b) enhanced image; (c) suppressed image ($a = -5 \times 10^{-5}$); (d) suppressed image ($a = -3 \times 10^{-5}$); (e) average score of "perceptual gloss"; (f) average score of "unnaturalness".

with this model, the light observed at position x can be decomposed into the light reflected on the front surface (surface I) and transmitted light from the back surface (surface II). Furthermore, this model assumes that the reflected light on surface I can be decomposed into specular and diffuse reflection components. The spectral distribution $S(\theta, \lambda, x)$ at position x is then represented by

$$S(\theta, \lambda, x) = c_D(\theta, x) S_D(\lambda) + c_S(\theta, x) + c_T(\theta, x) \tau(\lambda) S_T(\lambda), \quad (19)$$

where $c_D(\theta, x)$, $c_S(\theta, x)$, and $c_T(\theta, x)$ represent the geometric scale factors. $S_D(\lambda)$, $\tau(\lambda)$, and $S_T(\lambda)$ are the spectral reflectance of the diffuse reflection component, spectral transmittance, and spectral distribution of light incident from surface II, respectively. In other words, the first term on the right-hand side represents the diffuse reflection component, the second term indicates the specular reflection component, and the third term represents the transmitted components. The model assumes that the surface-spectral reflectance function at any incident angle is expressed by combining these three extremes. In this model, transparent objects and translucent objects can be described according to the strength of the diffuse + internal reflection component. In this paper, a transparent object with a small diffuse + internal reflection component is also called a translucent object. Equation (19) is expressed as an RGB three-dimensional vector as follows:

$$\begin{pmatrix} R \\ G \\ B \end{pmatrix} = c_D(\theta, x) \begin{pmatrix} \gamma_R \\ \gamma_G \\ \gamma_B \end{pmatrix} + c_S(\theta, x) \begin{pmatrix} 1 \\ 1 \\ 1 \end{pmatrix} + c_T(\theta, x) \begin{pmatrix} \rho_R \\ \rho_G \\ \rho_B \end{pmatrix}, \quad (20)$$

where $(\gamma_R \gamma_G \gamma_B)^T$ and $(\rho_R \rho_G \rho_B)^T$ represent the spectral reflectance of the diffuse reflection component and the spectral distribution of the transmitted light in the RGB color space, respectively.

Each pixel represented by Eq. (20) has the same hue, saturation, and intensity properties as those of inhomogeneous objects. Therefore, with the proposed method, the intensity of the specular reflection component is detected as a gloss for translucent objects. Note that translucent objects are affected by transmitted light; hence, even the same object may have different hue values. In addition, unlike inhomogeneous and metal objects, the saturation–intensity relationship may be proportional such that it does not pass through the origin.

4. EXPERIMENTS

This section presents the results of the application of the proposed method (The executable file is available at https://github.com/YManabe-ChibaUniv/GlossEditing.git) to test images. We also compared the proposed method with band-sifting algorithm.

Table I. Skewness of luminance histogram, contrast, and perceived contrast of test image "banana."

	Skewness	Contrast	Perceived contrast
(a) Input image	−1.04	29.44	–
(b) Enhanced image	−0.79	30.79	17.14
(c) Suppressed image	−1.09	29.24	−2.14

Figure 7 shows the results applied to a test image of "banana," which is generally represented using the dichromatic reflection model. To simplify the effect for easier understanding, the value of constant a, shown in Eq. (10), was set to $a = 15 \times 10^{-5}$ for gloss enhancement and $a = -5 \times 10^{-5}$ for gloss suppression. Table I shows the skewness of the luminance histograms, contrast, and perceived contrast. As shown in Fig. 7, only the glossy part was edited without changing the color of the diffuse reflection component. According to [16], the glossiness is highly correlated with the skewness of the luminance histogram, and many glossy objects produce a positively skewed luminance histogram. However, we need to be aware that an image with a positively skewed luminance histogram is not necessarily a glossy image [17]. Since the skewness of the luminance histogram alone is insufficient to explain gloss perception, studies [18–20] have used the contrast feature which has a high contribution rate in gloss perception. Therefore, we also verified the contrast as an objective evaluation. The contrast is defined as the standard deviation divided by the mean of the luminance histogram [20]. One study [19] also discussed the relationship between the "perceived contrast" and perceived gloss. Therefore, a psychophysical experiment was conducted to evaluate the perceived contrast on seven subjects at a rate of 0 to 100. The "perceived contrast" in Table I represents the average difference between the evaluation values of the input image and after gloss editing.

As shown in Table I, the skewness, contrast, and perceived contrast of the image with enhanced gloss were larger than that of the suppressed image. These results show that the proposed method can properly edit the gloss of an inhomogeneous object. Figures 8 and 9 show the results applied to test images of "coins" as a metallic object and "glass" as a translucent object, respectively. The results for these images with a scale factor of $a = -3 \times 10^{-5}$ are also shown in the figures. Tables II and III show the results of calculating the skewness from their luminance histograms, contrast, and perceived contrast. The results show that the proposed method can also properly edit the gloss of metallic and translucent objects.

As a subjective evaluation, an experiment was conducted in which seven subjects were asked to evaluate the "glossiness" and "unnaturalness" of the images. The reason why "unnaturalness" was checked for evaluation is that the proposed method and band-sifting may produce visible artifacts. The subjects were students, and the evaluation was

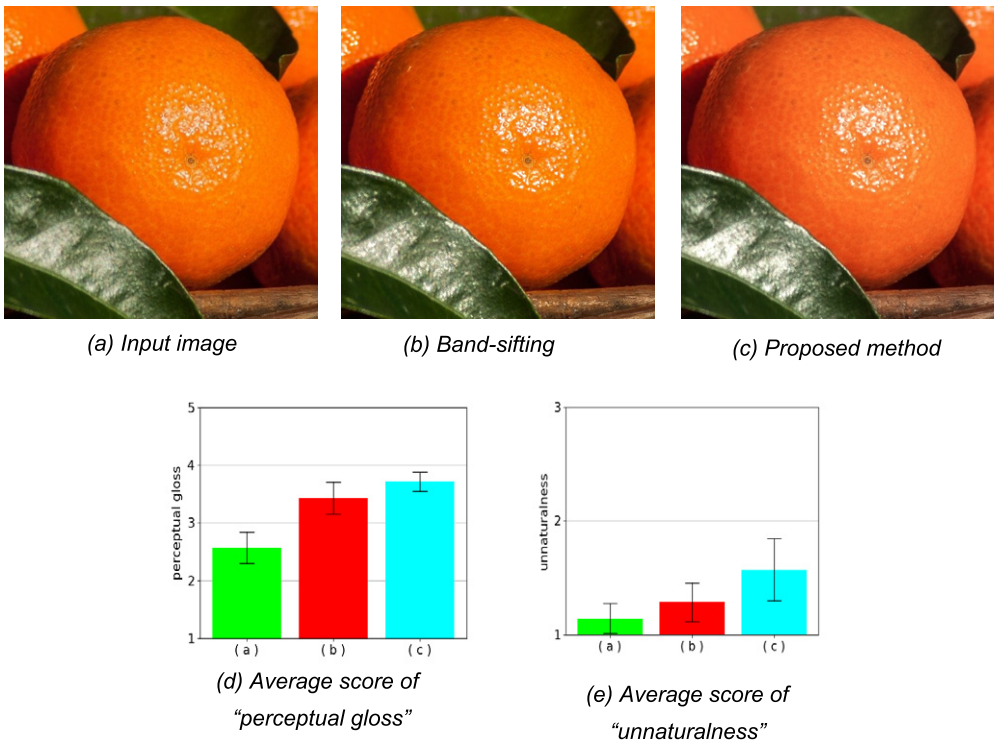

(a) Input image (b) Band-sifting (c) Proposed method

(d) Average score of "perceptual gloss" (e) Average score of "unnaturalness"

Figure 10. Results of glossy appearance enhancing for "orange." (a) input image; (b) band-sifting; (c) proposed method; (d) average score of "perceptual gloss"; (e) average score of "unnaturalness".

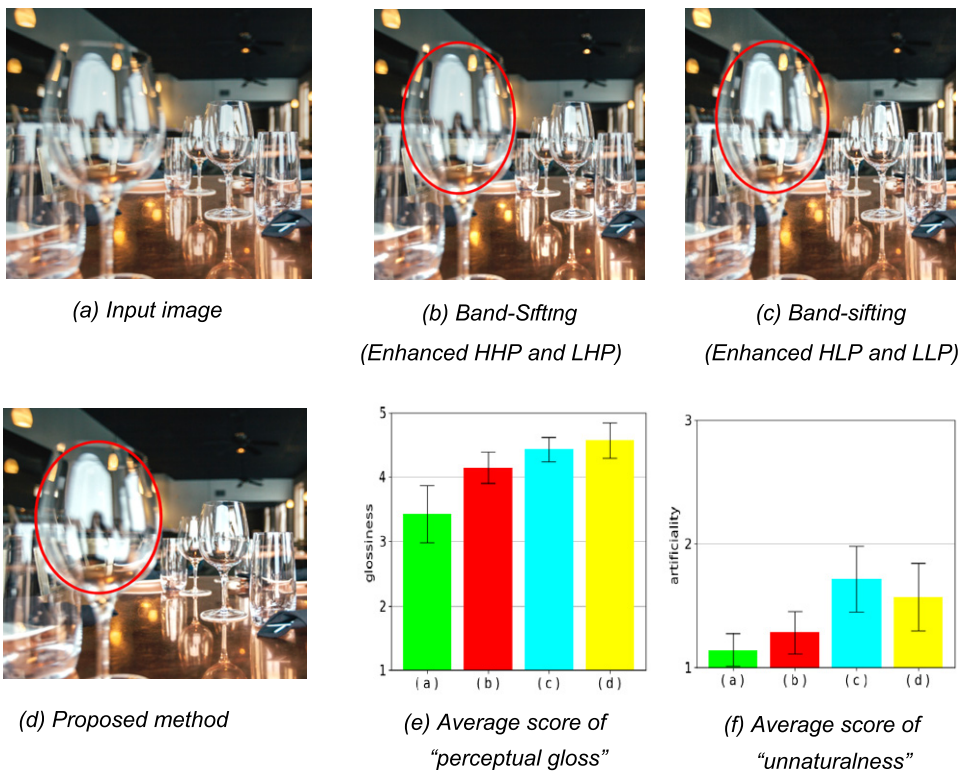

(a) Input image (b) Band-Sifting (Enhanced HHP and LHP) (c) Band-sifting (Enhanced HLP and LLP)

(d) Proposed method (e) Average score of "perceptual gloss" (f) Average score of "unnaturalness"

Figure 11. Results applied to a test image with large flat highlights. (a) input image; (b) band-sifting (Enhanced HHP and LHP); (c) band-sifting (Enhanced HLP and LLP); (d) proposed method; (e) average score of "perceptual gloss"; (f) average score of "unnaturalness".

(a) Input image (b) Proposed method (c) Band-sifting

Figure 12. Results applied to a test image with a high intensity background. (a) input image; (b) proposed method; (c) band-sifting.

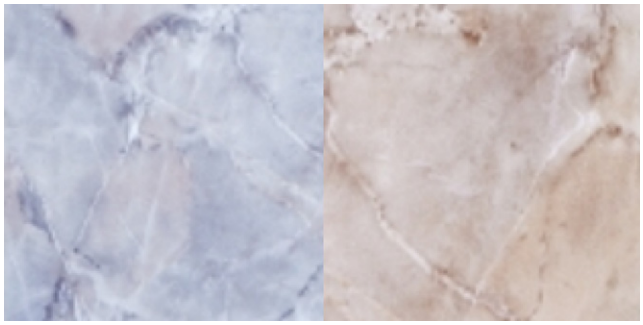

(a) Input image

(b) Enhanced image

Figure 13. Results of glossy appearance enhancing for "marble" with white texture. (a) input image; (b) enhanced image.

Table II. Skewness of luminance histogram, contrast, and perceived contrast of test image "coins."

	Skewness	Contrast	Perceived contrast
(a) Input image	0.07	60.18	–
(b) Enhanced image	0.16	63.54	10.14
(c) Suppressed image ($a = -5 \times 10^{-5}$)	−0.47	53.31	−13.57
(d) Suppressed image ($a = -3 \times 10^{-5}$)	−0.17	57.53	−7.14

Table III. Skewness of luminance histogram, contrast, and perceived contrast of test image "glass."

	Skewness	Contrast	Perceived contrast
(a) Input image	−0.83	35.84	–
(b) Enhanced image	−0.78	37.96	10.14
(c) Suppressed image ($a = -5 \times 10^{-5}$)	−1.41	30.47	−16.43
(d) Suppressed image ($a = -3 \times 10^{-5}$)	−0.63	33.82	−4.43

conducted by observing the images on the display at any viewing distance. Here, "glossiness" refers to the shining appearance of the object surface. "Unnaturalness" refers to the appearance of an object that does not exist in reality and is contrary to nature. The subjects were asked to rate the glossiness on a five-point scale, with 1 indicating no glossiness and 5 indicating very strong glossiness. They were asked to rate the unnaturalness of the image on a three-point scale, with 1 indicating a natural image and 3 indicating an unnatural image. The evaluation values for glossiness and unnaturalness are shown in Figs. (d) and (e), respectively. The results for the glossiness show that the scale factor of the proposed method is correlated with glossiness. This indicates that the proposed method is effective for glossiness. However, the method only considers glossiness and ignores other textures; for example, excessive gloss suppression may cause unnaturalness, as shown in the result for image (c) in Figure 8.

Several test images were used to compare the proposed method with band-sifting. Figure 10 shows the results applied to a test image of "orange." According to [7], gloss is enhanced by amplifying the high-frequency high-amplitude positive-sign (HHP) and low-frequency high-amplitude positive-sign (LHP) components. The HHP and LHP components are amplified as band-sifting parameters

(a) Input image (b) Enhanced image (c) Suppressed image

Figure 14. Results applied to a white object. (a) input image; (b) enhanced image; (c) suppressed image.

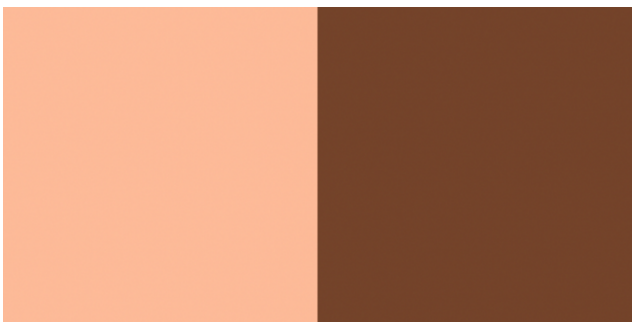

(a) Input image

(b) Enhanced image

Figure 15. Results applied the gloss detection processing to image containing the same hue. (a) input image; (b) detected gloss component.

to emphasize the dotted gloss of the orange surface and the flat gloss of the leaf surface. In the case of images with small highlights, such as dotted gloss, we adjusted the scale factor a of the proposed method while comparing them with images whose gloss was enhanced by amplifying the HHP and LHP components. As a result, there was no significant difference between the two images with enhanced gloss in term of both perceptual gloss and unnaturalness from Figs. 10(d) and 10(e).

Figure 11 shows the results applied to a test image with large flat highlights. As shown in Fig. 10, the HHP and LHP components of the band-sifting parameters are amplified. Although the glass in the foreground has a large flat gloss, band-sifting does not detect or emphasize the gloss. To enhance the gloss of these highlights, the HLP and LLP components need to be amplified. By emphasizing the highlights of the glass in the foreground, the gloss evaluation value is improved compared to the gloss enhancement process, which amplifies the HHP and LHP components. However, the disadvantages of gloss enhancement by amplifying HHP and LHP components [7] are the lack of consistent gloss enhancement and the increase in the evaluated unnaturalness. In contrast, the proposed method emphasizes large highlights. The proposed method is effective for images containing large highlights that cannot be detected as LHP components.

5. LIMITATION

In this section, we discuss the limitations of the proposed method.

Figure 12 shows the results applied to a test image with a high intensity background. When band-sifting is used to enhance the gloss, only the gloss of glass, ice, and metal pipes is emphasized, whereas the background is not. The proposed method also emphasizes the high intensity background area, and thus the visibility of the glass is reduced. In the case of a high intensity background, with the proposed method, both the main object in the image and the background are emphasized at the same amount, and thus the visibility of the main object may deteriorate, which is a drawback of the proposed method.

The proposed method alone cannot distinguish whether the white high-intensity regions on the object surface represent glossy components (such as specular reflection components) or surface texture (such as texture color or scratches on the objects). The “marble” image shown in Figure 13 has a white texture, but the gloss enhancement process of the proposed method emphasizes the white region. This indicates that the white texture is extracted as a glossy component. Because the proposed method uses the S-I plane for gloss detection, it is theoretically impossible to stably extract gloss from achromatic objects such as white objects. However, even objects that appear white are often not completely achromatic, and if they can be hue-segmented as colored, the proposed method is effective as shown in Figure 14.

In the hue-based segmentation of the preprocessing of the proposed gloss detection method, incorrect regions may be detected as gloss if the objects are made of different materials and have the same hue. Figure 15 shows the result of obtaining the gloss component using the proposed

(a) Input image (b) Enhanced image (c) Suppressed image

Figure 16. Results of glossy appearance editing for "clouds." (a) input image; (b) enhanced image; (c) suppressed image.

(a) Input image (b) Enhanced image (c) Suppressed image

Figure 17. Results of glossy appearance editing for "fireworks." (a) input image; (b) enhanced image; (c) suppressed image.

(a) Input image (b) Enhanced image

Figure 18. Result of gloss enhancement for an image with scratches. (a) input image; (b) enhanced image.

method for images containing the same hue. The difference in intensity values between the left region and the right region results in the left region being detected as gloss, as shown in Fig. 15(b), even though it does not have a gloss component.

When the intensity value of a glossy pixel in the input image has the maximum luminance, the proposed method cannot be expected to increase the gloss. The proposed method cannot edit the pixel with the maximum intensity, because the pixel value is changed in one direction when editing gloss. To improve perceptual gloss for input images where glossy pixels are already at maximum intensity or where gloss is very high, it is necessary to edit pixels with low gloss components rather than pixels with high gloss components, since contrast is a factor in gloss perception. In addition, the proposed method only considers glossiness, and editing only perceptual gloss independently from other attributes is an intrinsic and difficult problem. While we attempt to control physical properties directly, it is empirically known that changes in physical properties generally affect multiple visible attributes. In order to change only certain visible attributes, it is considered necessary to cancel the effects of other attributes by manipulating multiple physical properties.

Examples of the proposed method applied to clouds and fireworks are shown in Figs. 16 and 17 respectively. As shown in the figures, no significant change in glossiness is perceived for each image. This is because the proposed method is constructed based on the reflection and transmission models of the objects, which means that it does not cause significant effects on the glossiness of other phenomena. In order to edit the glossiness of those phenomena, it is necessary to construct a new gloss extraction model.

In the proposed method, scratches and artifacts on the object surface can be detected as gloss. Figure 18 shows the result of gloss enhancement on an image with intentional scratches on the object surface. In addition, Figure 19 shows the result of gloss enhancement processing on an image with block noise added by JPEG encoding. The results in Fig. 18 show that even noisy regions are extracted and emphasized as glossy components. If the glossy area of an image is degraded by block noise before applying the proposed method, the proposed method cannot enhance the glossy area. The area indicated by the blue frame in Figure 19 shows a large degradation of the glossy area during JPEG

(a) Input image (b) JPEG encoded image (c) Enhanced image

Figure 19. An example of gloss degradation due to block noise. (a) input image; (b) JPEG encoded image; (c) enhanced image.

encoding. Therefore, there is no significant change before and after the application of the proposed method, because the glossiness was degraded by a process different from the glossiness intensity by the reflection model. For images that contain a lot of noise, it is necessary to remove the noise in a preprocessing.

6. CONCLUSIONS

In this study, we proposed a method for editing the gloss of various glossy objects in a single image based on the reflection characteristics. The proposed method consists of three steps: color space transformation, gloss detection, and gloss editing. In the color space transformation, to detect the gloss of the object in the image, the color space is transformed such that the reflection characteristics of the object can easily be extracted. In gloss detection, the glossy region and gloss intensity are extracted based on the characteristics of the color space and the reflection characteristics of various materials. Gloss editing is conducted by editing the intensity of the extracted gloss. Using the above procedure, we were able to generate an image in which only the shiny areas were edited without changing the color of the non-shiny areas.

We analyzed the proposed method based on various reflection characteristics and determined that the gloss editing process edited the specular reflection component of inhomogeneous and translucent objects and the grazing reflection component of metallic objects. By applying the proposed method to test images, the effectiveness was confirmed not only through a visual evaluation but also in terms of the statistical image features.

As discussed in the previous section, the proposed method cannot improve the intensity value of an image containing the maximum intensity or an image that already contains high gloss by gloss enhancement processing. In order to improve glossiness more, it is necessary to consider contrast in gloss enhancement method since contrast is a factor of gloss perception. In addition to contrast considerations, editing of color factors such as saturation is also considered important in the pursuit of realism. Studies [20–22] have demonstrated the importance of the Fresnel effect in the perception of gloss. At present, the proposed method cannot induce the Fresnel effect because it does not obtain the shape of the object or the normal vector. However, the Fresnel effect can be enhanced if pixels in the region where the Fresnel effect is observed as a gloss component are detected during the gloss detection process. For images of inhomogeneous dielectric materials, where the color of the illumination light can be estimated from the specular reflection component, adding the color of the illumination light to the edge of the object may enhance the Fresnel effect and lead to improved results. Resolving these issues is future challenges.

REFERENCES

[1] A. C. Chadwick and R. W. Kentridge, "The perception of gloss: A review," Vis. Res. **109**, 221–235 (2015).
[2] F. B. Leloup, G. Obein, M. R. Pointer, and P. Hanselaer, "Toward the soft metrology of surface gloss: A review," Color Res. Appl. **39**, 559–570 (2014).
[3] F. B. Leloup, M. R. Pointer, P. Dutré, and P. Hanselaer, "Geometry of illumination, luminance contrast, and gloss perception," J. Opt. Soc. Am. A **27**, 2046–2054 (2010).
[4] F. B. Leloup, M. R. Pointer, P. Dutré, and P. Hanselaer, "Overall gloss evaluation in the presence of multiple cues to surface glossiness," J. Opt. Soc. Am. A **29**, 1105–1114 (2012).
[5] J. R. Cheeseman, J. A. Ferwerda, F. J. Maile, and R. W. Fleming, "Scaling and discriminability of perceived gloss," J. Opt. Soc. Am. A **38**, 203–210 (2021).
[6] ITU-T T.81, "Information technology – Digital compression and coding of continuous-tone still images - Requirements and guidelines".
[7] M. Tanaka, T. Takanashi, and T. Horiuchi, "Glossiness-Aware Image Coding in JPEG Framework," J. Imaging Sci. Technol. **64**, 050409-1–050409-15 (2020).
[8] M. Tanaka and T. Horiuchi, "Investigating perceptual qualities of static surface appearance using real materials and displayed images," Vis. Res. **115**, 246–258 (2015).
[9] M. Tanaka, R. Arai, and T. Horiuchi, "PuRet:Material appearance enhancement considering pupil and retina behaviors," J. Imaging Sci. Technol. **61**, 040401-1–040401-8 (2017).
[10] I. Boyadzheiev, K. Bala, S. Paris, and E. Adelson, "Band-sifting decomposition for image based material editing," ACM Trans. Graph. **34** (2015).
[11] D. Miyazaki, R. Tan, K. Hara, and K. Ikeuchi, "Polarization-based inverse rendering from a single view," *Proc. Int'l. Conf. on Computer Vision* (IEEE, Piscataway, NJ, 2003), pp. 982–987.
[12] R. Bajcsy, S. Lee, and A. Leonardis, "Detection of diffuse and specular interface reflections and interreflections by color image segmentation," Int. J. Comput. Vis. **17**, 241–272 (1996).
[13] T. Higo, D. Miyazaki, and K. Ikeuchi, "Realtime removal of specular reflection component based on dichromatic reflection model," IPSJ SIG Technical Report (2006), 2006, pp. 211–218, (in Japanese).
[14] S. Tominaga and B. A. Wandell, "Standard surface-reflectance model and illuminant estimation," J. Opt. Soc. Am. **6**, 576–584 (1989).

[15] S. Tominaga, "Dichromatic reflection models for a variety of materials," Color Res. Appl. **19**, 277–285 (1994).
[16] I. Motoyoshi, S. Nishida, L. Sharan, and E. H. Adelson, "Image statistics and the perception of surface qualities," Nature **447**, 207–209 (2007).
[17] B. L. Anderson and J. Kim, "Image statistics do not explain the perception of gloss and lightness," J. Vis. **9**, 1–17 (2009).
[18] P. J. Marlow, J. Kim, and B. L. Anderson, "The perception and misperception of specular surface reflectance," Curr. Biol. **22**, R865–R866 (2012).
[19] P. J. Marlow and B. L. Anderson, "Generative constraints on image cues for perceived gloss," J. Vis. **13**, 1–23 (2013).
[20] M. Toscani, D. Guarnera, C. Guarnera, J. Y. Heardeberg, and K. Gegenfurtner, "Three perceptual dimensions for specular and diffuse reflection," ACM Trans. Appl. Perception **17**, 1–26 (2020).
[21] F. Faul, "The influence of Fresnel effects on gloss perception," J. Vis. **19**, 1–39 (2019).
[22] F. Faul, "Perceived roughness of glossy objects: The influence of Fresnel effects and correlated image statistics," J. Vis. **21**, 1–29 (2021).